An Artificial Intelligence Model for Enhancing The State of Charge Prediction in Electric Vehicles Batteries

Raid Mohsen Alhazmi[*]

University of Tabouk, Computer Science, Tabouk, Saudi Arabia

* Corresponding author; E-mail: ralhazmi@ut.edu.sa

Abstract:

Electric vehicles (EVs) have implemented lithium-ion batteries (LIBs) due to their remarkable energy density and avoidance of environmental pollution. The State of Charge (SOC) is an important statistic that reflects the remaining charge in the battery, and its exact assessment is essential for Battery Management System (BMS) and improving EV efficiency, which extends the battery's life and decreases the probability of catastrophic failure. Hence, this paper employs a Deep Learning (DL) algorithm to enhance the estimation accuracy of SOC to obtain accurate SOC measurements. This research introduces the Temporal Fusion Transformer Integrated with Bayesian Optimization Algorithm (TFT-BOA) model for enhancing feature extraction and classification performance. The BMW i3 EV dataset is utilized for training the model for better results. The data collected from the dataset is pre-processed using the normalization method called min-max. TFT is used for feature extraction and classification of pre-processed data. BOA is used to tune the hyperparameters of TFT to enhance prediction precision. The dataset was further divided for training & testing of the model. The performance of the TFT-BOA model is calculated using the Mean Absolute Percentage Error (MAPE), Mean Absolute Error (MAE), Mean Squared Error (MSE) and Root MSE (RMSE) metric values. The proposed model generates accurate results for SOC prediction, with all RMSEs being within 0.16%, MAEs being within 0.035%, MSEs being within 0.15%, and MAPEs being within 2%. The average values of RMSE, MAE, MSE, and MAPE are 0.13, 0.024, 0.10, and 1.13 respectively. Experiments confirmed that the Temporal Fusion Transformer with Bayesian Optimization Algorithm (TFT-BOA) model has the highest accuracy among those that predict the SOC.

Key words: Electric Vehicle, State-of-Charge, Lithium-Ion Batteries, Deep Learning, TFT, BOA.

1. INTRODUCTION

Recent years have witnessed an increase in the popularity of EVs. Broad acceptance of EVs signifies a progression in the growth of both public and private transportation, given the current state of research and development and the constant advancement of technology. Secondly, one of the primary

contributors to CO2 emissions, which is a critical factor in climate change, is the transportation sector, Pevec et al. (2019). The initial EV demo took place in 1838, and the first mass-produced EV was introduced in 1884 Miao et al. (2019). Since the beginning of the twenty-first century, environmental contamination and energy-related issues have been cited as the main reasons behind the rapid growth of EV research. EV technology and infrastructure have been improved because of the collaboration between the government and industry. In 2016, one million EVs were sold worldwide; by 2018, that number had surpassed five million, for both plug-in hybrid electric vehicles and light-duty EVs. Volkswagen, Mercedes-Benz, and Ford, among other well-known automakers, have expressed their desire to promote EVs Sun et al. (2019). In the United States, yearly sales of electric and hybrid vehicles increased from 0.6% to 4%; in Norway, a country with a significant EV market share, this figure has risen to 86% by 2022 Thangavel et al. (2023). Figure 1 shows that EV sales doubled in 2021.
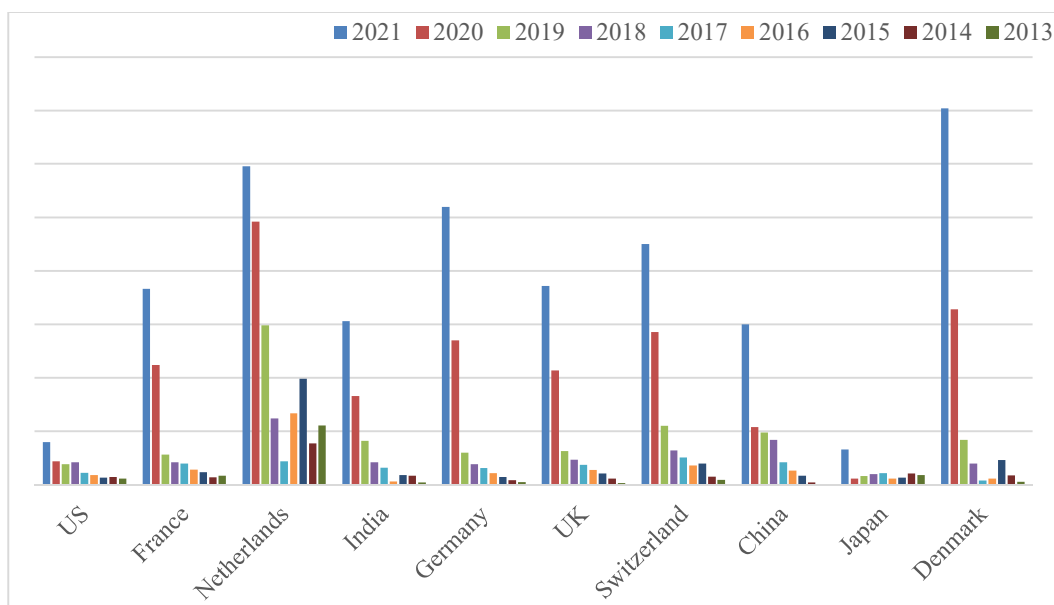

Figure 1. Statistical Analysis of EV by Country (Thangavel et al. 2023)

Large-scale deployment of EVs requires substantial adjustments to existing automakers, with the electricity storage system, or battery, being the most essential component of an EV. Presently, the sector is preoccupied with LIBs, a technological advancement that has demonstrated its dependability and the potential for cost reductions due to premium manufacturing Stampatori et al. (2020). The growing interest in LIBs can be attributed to their significant potential in delivering energy storage efficiency and promoting environmental sustainability. At present, LIBs find applications not only in compact electronic devices like cell phones and computers but as well as in electric or hybrid automobiles Chen et al. (2020). LIBs market opportunities have been growing. It is anticipated that the LIBs market will reach a valuation of USD 90.01 billion by 2024. Between 2020 and 2026, the market of sales is projected to increase at a Compound Annual Growth Rates (CAGR) of 20%, owing to a growing EV sector, declining LIBs prices, the shift towards intelligent electronics, expanding smart wearables shipments, and robust demand for consumer electronics declining LIBs prices Rangarajan et al. (2022). The valuation of the worldwide LIBs market in 2021 was USD 58.61 billion. It is anticipated

that this figure will increase at a CAGR of 18.9% between 2022 and 2030, reaching USD 278.27 billion by 2030.
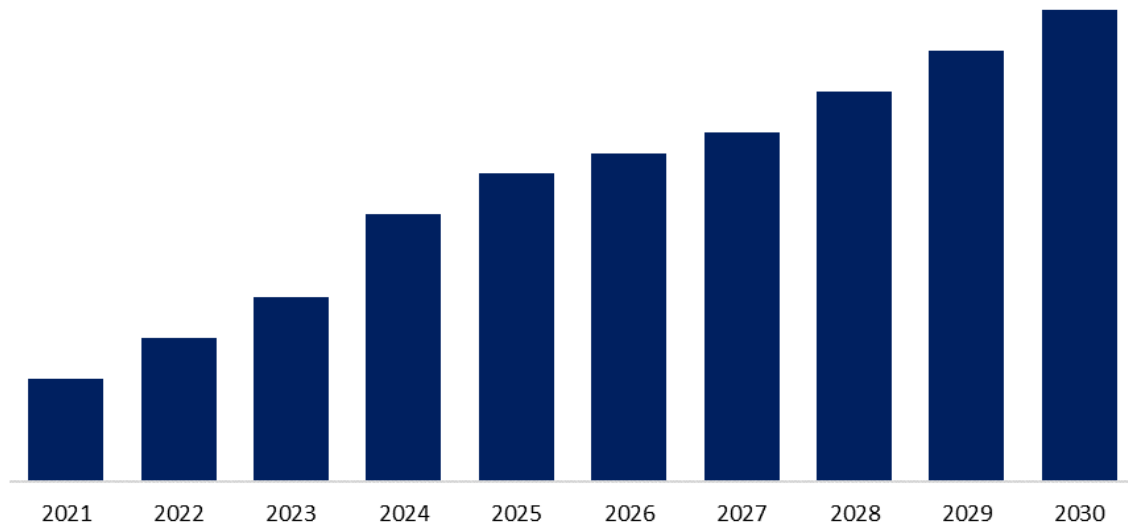

Figure 2. Size of lithium-ion batterries market (Rangarajan et al. 2022).

In addition to batteries, effective battery management is critical for EV batteries to function reliably and safely. Collection of battery data, determination and prediction of battery status, control overcharge and discharge, thermal management, balance control, safety protection and communication are all essential components of a comprehensive BMS Thangavel et al. (2023). An electronic device known as a BMS is essential for monitoring and regulating the performance of EV batteries. Voltage, temperature, and SoC are critical parameters that dictate the safe operation of batteries that are frequently found in EVs. Real-time information on critical battery parameters such as temperature, current and voltage is retrieved by the BMS. By utilizing these metrics, BMS constantly observe critical performance parameters like State of Health (SoH), which indicates the general condition of the battery pack, and SoC, which represents the remaining charge beyond the utmost capacity of the EV battery. Monitoring the SOC enables owners of EVs to estimate their free driving range and schedule charging station visits with minimal concern for range anxiety. By implementing SoH monitoring, EV manufacturers could effectively support their consumers by offering advance notice of necessary maintenance, ensuring optimal battery health, and extending overall performance. There are numerous substantial benefits associated with BMS for EVs. Performance optimization, safety and dependability, and real-time data diagnostics are among these advantages. A synopsis of BMS is illustrated in Figure 3.
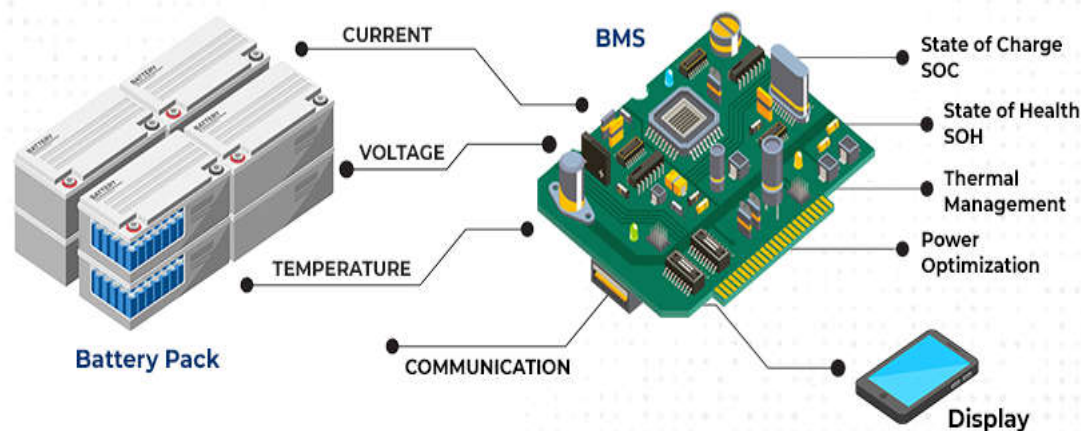
Figure 3. Overview of Battery Management System

As an indicator of the battery's remaining power that enables the computation of other EV quantities, the SOC is a more significant parameter among the LIB's state parameters. It is comparable to the quantity of petroleum in a gasoline-powered vehicle. SOC parameters are the primary focus of this study. Physical quantification and accurate assessment of SOC with instruments are not possible Saldana et al. (2019). At present, an estimation of SOC is typically accomplished by parameter measurements that exhibit a robust correlation, such as voltage, charge, temperature, capacity, current and so forth Zhang et al. (2022). However, the reflection of electrochemical in LIBs is a complex process that is highly vulnerable to temperature fluctuations and material fatigue Saldana et al. (2019). The relation between the current state battery capacity and the entire charge capacity of the battery is represented by the specific mathematical equation (1).

$$SOC = \frac{C_{current}}{C_{now}} \times 100 \qquad (1)$$

Here, $C_{current}$ is the battery capacity in real-time, and C_{now} is the fully charged condition. The SOC of a battery completely charged is 100% when it reaches 0% upon completion of battery discharge Sun et al. (2019). In the real-time implementation of BMS within EVs, the calculation method of SOC serves as the foundation for the mathematical representation of SOC Zhang et al. (2022).

This research mainly focuses on developing a deep-learning model capable of accurate SOC prediction. When compared to traditional feature engineering methods, DL models possess the capability to independently obtain hierarchical representations of input features from unprocessed data. DL models can scale to handle large datasets efficiently, which is crucial for SOC prediction tasks that may involve extensive historical data from battery sensors. Additionally, DL frameworks offer tools for distributed computing, enabling models to be trained on parallel computing resources for improved scalability. The basic work model of DL-based SOC prediction of EV is illustrated in the figure 4.
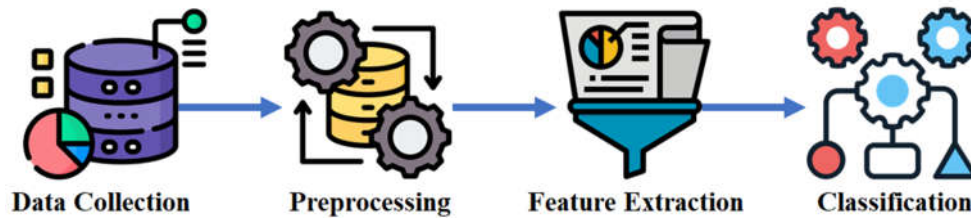
Figure 4. Basic Workflow of the SOC Battery Prediction Model.

The model's fundamental workflow comprises the subsequent phases: collecting datasets, pre-processing of data, extraction of features, classification, and analysis of SOC prediction. The initial phase consists of gathering real-time data from the dataset. The gathered data undergoes pre-processing to eliminate extraneous and noisy components. Subsequently, the pre-processed data is sent into the feature extraction and classification stage. The implementation of a DL model for classification will enhance the model's efficiency. Following the classification procedure, SOC parameters at varying temperatures are computed.

1.1. Research Objectives

The research objectives for this work on SOC prediction using the TFT + BOA model can be outlined as follows:

- To construct a novel hybrid model involving feature extraction and classification to forecast SOC.
- To improve the pre-processing methodology of a model, the normalisation technique is employed.
- To enhance the efficacy of SOC prediction by implementing the TFT algorithm, which is utilized to extract and classify features.
- In this investigation, the optimization of hyperparameters by employing the BOA improves the efficiency of the TFT model.
- To assess the effectiveness of the TFT + BOA model using a real-time dataset obtained from the BMW i3 electric car.
- To assess its performance utilising the parameters MAE, RMSE, MAPE and MSE metric values.
- To evaluate the effectiveness of the proposed model in improving SOC prediction by comparing the performance of the TFT+BOA model to that of other approaches that were reviewed.

In contrast to model-based and data-driven approaches, this paper concludes that the SOC prediction method based on the TFT+BOA is the most suitable strategy following an exhaustive review of numerous prediction methods in the existing literature. Particularly for diagnostics and modelling purposes, the BMW i3 EV dataset contains information regarding the lithium batteries utilized in battery EVs. For the processing of data gathered from the data set, min-max normalization is implemented. TFT classification is performed using the collected data from the datasets following pre-processing. The Bayesian Optimization algorithm is also employed to fine-tune the hyperparameters of TFT. By integrating the TFT and BOA, this article presents an improved SOC prediction model for LIBs.

2. RELATED WORKS

This segment provides a detailed analysis of current works developed and proposed for the estimation and prediction of SOC. A Least Squares Support Vector Machine (LSSVM) was employed in Li et al. (2020) to construct the battery model to reduce the model's dependency on the battery's intrinsic parameters. The parameters of the model were optimized utilizing the GWO algorithm to enhance the estimation performance of LSSVM. The benefits of the enhanced model were then validated using the CV algorithm. Additionally, the LSSVM model utilizing the sliding window was suggested as a means to enhance the estimation accuracy of SOC. By comparing the model to alternative estimators, its efficacy is ultimately validated across a range of driving conditions and temperatures. As evidenced by the reduction in RMSE from 0.89% to 0.22% and the ability to control the MAE to within 1%, the comparison results validate the model's effectiveness and robustness.

For battery SoC estimation, Xiao et al. (2019) introduced a gated recurrent unit (GRU) based recurrent neural network (RNN) model. A combined optimization technique utilizing the AdaMax optimizers and Nadam permits the GRU-RNN model to acquire knowledge of its parameters promptly. In the pre-training phase of the model, the Nadam optimizer was employed to quickly determine the minimum optimized value. Following that, during the model fine-tuning phase, the AdaMax optimizer was utilized to refine the model parameters. Ultimately, a novel approach for estimating the SoC of a battery was introduced: the GRU method. This method solely necessitates data samples for model training and can generate precise and efficient SoC estimates. The framework was trained and evaluated utilizing three distinct dynamic loading profiles in order to determine the efficacy and reliability of the model. Subsequently, the model was compared to well-established techniques utilized in the estimation of SoC. The RMSE, MAE, and MAPE metrics have respective mean values of 1.13%, 0.84%, and 3.28%. The study by Kumar et al. (2024) introduced the utilization of an optimized CNN model for estimating SOC. To enhance the CNN architecture, Elephant Search Algorithm (ESA), Equilibrium Optimization (EO) and Particle Swarm Optimization (PSO), were implemented. The key performance indicators that were assessed included MAE, MSE, MAPE, R2, and execution time measured in seconds. MSE was 0.362, MAE was 0.283, MAPE was 6.19, and R2 was 0.932, among other metrics, provided by the initial CNN model. With the highest performance metrics (MSE = 0.152, MAE = 0.075, and MAPE = 2.65), the ESA-CNN configuration executed exceptionally well. Moreover, at 0.9987, it exhibited the highest R2 value.

Predicting the discharge capability of LIB, the work by Vakharia et al. (2023) offered an exhaustive examination of a highly effective optimized Ex-AI model. A publicly available dataset on the aging of Li-ion batteries was utilized to construct the methodology. An evaluation was conducted on the prediction capability of 3 DL models, namely SRNN, GRU, and Stacked-LSTM, using feature selection via Ex-AI models. The discharge capacity of LIB was predicted more accurately by stacked LSTM than by GRU and SRNN DL models. It was discovered that the predictive capability of the features chosen after the application of jellyfish-optimized Ex-AI models was superior to that of both features combined. The findings indicate that the utilization of the jellyfish-Ex-AI model improved the accuracy of discharge capacity predictions. The methodology's efficacy was demonstrated by the extremely low RMSE (0.04), MAE (0.60%), and MAPE (0.03) values observed with the model. To accurately determine the SOC across a broad spectrum of temperatures in LIBs, the researchers Sherkatghanad et al. (2024) proposed CNN-Bi-LSTM-AM, a deep-learning model based on self-attention. To highlight the resemblance between input vector pairs, the method employed self-attention layers and a CNN architecture for extracting relevant features and a Bi-LSTM for capturing temporal characteristics, respectively. When compared to alternative DL networks, the model demonstrated a better overall performance. It was worth mentioning that during the 180-minute training period, the

model enabled to reduce the RMSE as well as the MAE to 1.27% and 0.75%, respectively, for these data.

To generate precise state-of-charge (SOC) estimates for LIB, Lipu et al (2020) introduced an enhanced data-driven algorithm that utilizes TDNN with iFA optimization. By determining the optimal values for UTD and HNs, the iFA algorithm significantly enhances the processing capability of TDNN. As a result, SOC accuracy and robustness were both improved. Two distinct experiments—SDT and HPPC—were conducted to validate the completely developed algorithm using two distinct types of LIB cells. With a narrow SOC error of less than 5% in the SDT and HPPC experiments, this algorithm generates outstanding SOC estimation outcomes characterized by low parameter values. The algorithm's pre-eminence was further demonstrated by the SOC estimation outcomes at variable temperatures and EV drive cycles, with reported RMSE values of less than 1%. Additionally, the method can deliver superior solutions in terms of precision, efficiency, and robustness provided by a comprehensive comparison with existing SOC estimation techniques considering various temperatures.

The work by Huang et al. (2017) introduced a method for concurrently determining the state-of-health (SOH) and SOC of LIBs online that was both dependable and precise. By analysing cycle-life test of battery data, it was possible to derive the SOC equation's model parameters, which are the Immediate discharge voltage (V) and its unit time voltage decline, V0. 1/V0 multiplied by the modification factor, which was dependent on SOC, was determined to have a linear relationship with the SOH equation. As demonstrated by the outcomes, the model constructed using data from a solitary cell can estimate with SOC a 5% margin of error and SOH of the remaining three cells. The model's accuracy and prospective applicability in an EVs BMS are validated through a Test of random sampling that simulates online real-time SOC, SOH estimation. To assess the model's robustness, the outcomes revealed that employing any battery from the same batch for the model's construction produced identical levels of precision across all four cells.

To achieve greater accuracy, a model was constructed utilizing RNNs to acquire the suitable vector representation of battery information. Subsequently, the work by Zhao et al. (2020) proposed an Extended CNN (E-CNN)-based model that was supplied with the vector of battery that has been thoroughly trained. It was demonstrated that by incorporating these well-trained vectors into multi-channel E-CNN, this method improved the SOC prediction performance of batteries. The method was subjected to simulation using real-world datasets, and it was evaluated in comparison to several cutting-edge approaches. The results of simulations indicated that it outperforms recurrent neural networks by 4.3% and the Ah counting method by 11.3% with regards to prediction accuracy. The implementation of the RNNs-CNNs model in a real-time environment has become feasible with the advent of Edge Computing. To increase the performance of SOC estimation, the work by Lipu et al. (2018) suggested an enhanced recurrent NARXNN-based LSA model. LSA was applied to the NARXNN model to identify the global optimal solution. Highlighted below were the primary innovative aspects of this research: Implementing LSA improved the algorithm's computational intelligence; the algorithm operated efficiently without requiring complex mathematical equations and battery models; PSO was exceeded LSA in terms of achieving the minimum objective function; and PSO was compared to LSA to determine its efficiency. Lastly, by ignoring the time-consuming and ineffective techniques utilized by alternative approaches, the NARXNN-based LSA model conserves both human effort and time while maintaining a desirable level of accuracy and complexity.

The TCN network efficiently correlates current, temperature and voltage with the SOC of a battery, as detailed by Liu et al. (2021). The SOC of a LIB under varying temperatures and operating conditions can be approximated using a single model, which has a high degree of accuracy following training. Directly mapping battery measurement parameters to SOC was a more suitable method for the onboard system than the conventional approach, which necessitates the manual establishment of the

battery model or the calculation and determination of a substantial number of parameters. The estimation effect of the model's generalization to a real-world scenario was also evaluated concurrently with the model's performance being carefully validated using a publicly available data set. The error observed in the model estimate results was 4.64%, while the average MAE and RMSE were 0.39% and 0.61%, respectively. The implementation of SOC Estimation of LIBs Using LSTM and NARX was described by Wei et al. (2020). The time-unfolded model incorporates connections of jump-ahead made possible by the LSTM memory embedded in the hybrid NARX model. The empirical findings indicated that the model exhibited an estimation performance RMSE below 1%. Furthermore, it demonstrated superior performance in multi-time prediction. To calculate the performance of the hybrid model under dynamic stress test (DST) and urban dynamometer driving schedule (UDDS) conditions, it was compared to the BPNN-PSO and the LSTM existing models. The accuracy with which the hybrid NARX-LSTM model estimated the state of charge of the battery was superior to that of alternative methods. In comparison to the conventional LSTM, the model exhibited an approximate 60% improvement in RMSE.

Utilizing a dual fractional-order model (FOM) and extended Kalman filter (EKF), the research by Ling and Wei (2021) proposed a model for calculating the combined SOC, and SOH of LIB. The AGA method was utilized to implement the identification of offline parameters for the battery model during the HPPC test, and the identification accuracy was verified. In addition, the SOC is estimated utilizing an SFOEKF algorithm that is founded upon the offline identified parameters. A comparison analysis was done between the DFOEKF and SFOEKF models for estimating SOC under the FUDS, DST, and US06 specifications. Compared to the SFOEKF, which utilizes fixed parameters, the DFOEKF achieves a more precise SOC value through online parameter updates. As compared to the US06, FUDS and DST, experiments conducted at room temperature, the SOC RMSEs decreased from 6.87%, 8.50%, and 7.32% to 0.48%, 0.63%, and 0.86%, respectively.

2.1. Research Gap Analysis

Different machine learning (ML) models such as LSSVM, RNN, CNN, and TCN have been explored for SOC estimation. Techniques like parameter optimization using algorithms such as GWO, Nadam, AdaMax, PSO, ESA, and Equilibrium Optimization (EO) have been integrated to enhance model performance. Hybrid models combining different architectures such as NARX-LSTM and CNN-Bi-LSTM-AM have demonstrated superior performance in SOC estimation, showcasing advancements in combining diverse techniques for better accuracy and efficiency. Ensemble optimization techniques like an ensemble of Nadam and AdaMax optimizers have been utilized to refine model parameters and improve estimation performance. There is a gap in exploring more complex architectures or novel combinations of these architectures to further improve estimation accuracy, especially under diverse operating conditions and temperature variations. Future research could focus on systematically evaluating the effectiveness of various optimization algorithms in combination with different deep-learning models for battery state estimation. By establishing standardized and methodical algorithms utilizing the most effective optimization techniques, conducting a comprehensive evaluation of the performance of multiple algorithms, and placing a priority on interpretability, the proposed study will ultimately aid in the development of SOC prediction models for EVs. A comprehensive summary of previous studies is presented in the literature review, which also lays the foundation for the proposed method of enhancing SOC estimation capabilities.

3. PROPOSED METHODOLOGY OF THE TFT-BOA MODEL

This research proposes a model to improve battery SOC prediction in EVs by combining TFT-BOA for feature extraction and classification. By incorporating these techniques, the model aims to

resolve the challenges of battery prediction in EV environments and enhance detection accuracy. This research developed a novel TFT-BOA algorithm for predicting the SOC performance of LIBs in EVs. The model that has been presented consists of several stages: accumulation of datasets, pre-processing, feature extraction and classification. In the preprocessing stage, the normalisation technique is incorporated by using min-max normalisation to improve the model performance. TFT is used for feature extraction from the processed data and classification to minimize the complexity of the model. After classification, for tuning hyperparameters obtained in the TFT, the BOA algorithm is used algorithm for the effective output. The effectiveness of this TFT-BOA model is assessed across a range of temperatures using the BMW i3 EV dataset and is subsequently compared to pre-existing models. The TFT-BOA algorithm's overall workflow is depicted in Figure 5. It consists of the following stages: data collection, pre-processing, feature extraction and classification, parameter tuning, training, testing and performance measures. The following sections explain and discuss the implementation of these stages.

3.1. Dataset Details

The simulation experiments in this research will utilize a real dataset consisting of numerous journeys completed by a BMW i3 EV, having a 60 Ah battery pack. The information presented here was collected via the OBD interface using EV sensors that were installed on the vehicle. The sampling rate is 1Hz. Particularly, this data set includes missing values because of the additional factors or measurement errors. As a result, it is crucial to perform primary processing tasks to filter the initial data. Due to drive behavior, high-voltage batteries in battery EVs experience substantial load fluctuations. In contrast to this dynamic performance exhibited by the powertrain, the auxiliary consumers operate at an almost constant capacity. The heating and air conditioning system generates the most auxiliary power, which substantially reduces the vehicle's range. For model validation purposes, 72 actual driving journeys were recorded while operating a BMW i3 (60 Ah). These trips encompassed both the heating circuit and powertrain of the vehicle. Environmental (temperature, altitude, etc.), vehicle (speed, throttle, etc.), battery (voltage, current, temperature, SoC), and heating circuit (indoor temperature, heating power, etc.) data are included in each journey Sulaiman and Mustaffa (2024).

By applying TFT-BO to the dynamic data characteristics of the BMW i3 EV and utilizing real-world data, it is expected that accurate and significant SOC predictions will be generated, thereby making a valuable contribution to the progress of estimating battery state in EVs. Splitting the dataset for training and testing sets. For example, training can be conducted using travels #1 through #60, which aggregate to 945,027 instances. 118,974 instances comprise the testing dataset, which consists of trips #61 to #70. Additionally, the data set utilized in this work is available with open access at https://ieee-dataport.org/open-access/battery-and-heating-data-real-driving-cycles via IEEE Data port.

3.2. Data Preprocessing

Preprocessing is the initial stage of data preparation before applying any analysis or modelling techniques. It involves transforming raw data into a clean and usable format. Raw data can be messy and contain errors like inconsistencies, missing values, outliers, or irrelevant information. Preprocessing helps identify and rectify these issues, ensuring the data used for analysis is accurate and reliable. Preprocessing techniques like scaling or normalization can put different features on a similar scale, making it easier for analysis algorithms to process and interpret the data. This improves the efficiency and accuracy of subsequent modelling or analysis steps. Data normalization is a technique applied to datasets to improve their quality and prepare them for further analysis or modelling. In

general, normalization is implemented to facilitate optimal convergence in neural networks and reduce training time Liu et al. (2023).
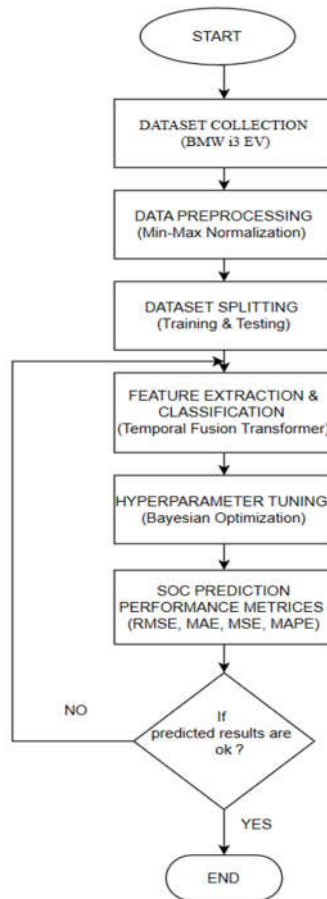

Figure 5. Workflow of the Proposed Model.

As a result of the dataset's diverse scales, this investigation applied MinMax scaling to standardize the scale of each feature. The application of MinMax scaling to the original data results in a linear transformation. The formula for scaling is given below, Liu et al. (2023):

$$x' = \frac{(x - min)}{(max - min)} \tag{2}$$

Where, the variable x denotes the original data and x' as transformed data. The maximum and minimal values of the column in which x is located are denoted as Min and max, respectively. The scope of this standardization method is extensive. Through the implementation of this approach, data are transformed into a range of [0, 1] while preserving their basic structure. Consequently, this methodology facilitates quick and simple data normalization, all the while sticking to a specified range.

3.3. Temporal Fusion Transformer Model for Feature Extraction and Classification

Attention-based deep neural networks are utilized to generate multi-horizon time series forecasts using the TFT. In this research, TFT is used for feature extraction and classification purposes. Although attention-based algorithms for forecasting time are prevalent, only a limited number of them exhibit exceptional accuracy and interpretability. By incorporating interpretable multi-head attention and altering the structural design of the initial transformer, TFT resolves this issue. Furthermore, TFT employs gating approaches to eliminate components unused and a network of selected variables to ascertain pertinent variables of input, thereby enhancing the precision of forecasts. Additionally, TFT stresses the importance of handling separate input variables, such as dynamic and static variables, independently Chang et al. (2021) and Ji et al. (2023).

The primary objective of the initial TFT model is to effectively extract observations from static data. We reduced the complexity of the TFT model, however, due to the absence of static data in the dataset. Consider the situation in which we try to predict the amount of energy consumed for the following t days using data from the previous k days. Future inputs that are known can then be distinguished from previous inputs. Inputs from the prior k days consist of consumption. Inputs that are known in advance are variables whose values and time indexes for the subsequent $tmax$ days are examples of known future inputs. The factors $tmax$ and t may differ in practice; however, for simplicity, we assumed that they were both equal in the experiment. In the TFT architecture, the utilization of Long Short-Term Memory (LSTM) encoders and decoders alongside the transformer components enables effective feature extraction from past inputs and known future inputs, respectively,

3.3.1. LSTM Encoders for Past Inputs:

Past inputs refer to the historical data of the EV's SOC leading up to the current time point. These past inputs are supplied to the series of LSTM encoders. LSTM is a type of RNN known for its ability to capture temporal dependencies in sequential data. The LSTM encoders process the past input sequences and extract meaningful features that capture patterns and dependencies in the historical SOC data.

3.3.2. LSTM Decoders for Known Future Inputs:

Known future inputs are the contextual information or exogenous variables available for future time points, such as weather forecasts, charging station availability, etc. These future inputs are also given to a sequence of LSTM decoders. The LSTM decoders extract relevant features from the known future inputs, providing additional context for predicting future SOC values.

3.3.3. Combination with Transformer

After feature extraction from both past and future inputs using LSTM encoders and decoders, respectively, the extracted features are combined with the transformer components. The transformer architecture, with its self-attention mechanisms and multi-head attention layers, effectively captures temporal dependencies and relationships across different time steps in the SOC data. By integrating LSTM-based feature extraction with the transformer architecture, TFT leverages the strengths of both methodologies to increase the robustness and accuracy of SOC prediction. The architecture of TFT is illustrated in Figure 6. To extract features, previous inputs are passed through a succession of LSTM encoders. Identical future inputs are also passed through a sequence of LSTM decoders to derive additional features. Local analysis of time-dependent inputs is performed by these LSTMs to compute

temporal self-attention. Designed to improve explainability, the temporal self-attention mechanism in transformer-based architectures is an altered form of multi-head attention. The attention, or the significance of the features of each vector in the input, is assessed by this module through the utilization of 3 variables. Before calculating temporal self-attention, the Add&Norm and Gate layers analyze the concealed states of LSTMs. The gating layer is denoted by the Gate layer and is constructed using GLUs Ji et al. (2023). Gating layers offer the advantage of allowing for the suppression of any architectural components that are considered unnecessary for a specific dataset. The mathematical representation of GLUs is denoted by Equation (3), in which X signifies the input of the Gated Linear, W_1, W_2 denote the learnable weight matrix parameters, b_1, b_2 represent the following bias parameters, σ (.) indicates the activation functions of sigmoid, and $\odot$ signifies the Hadamard products element-wise.

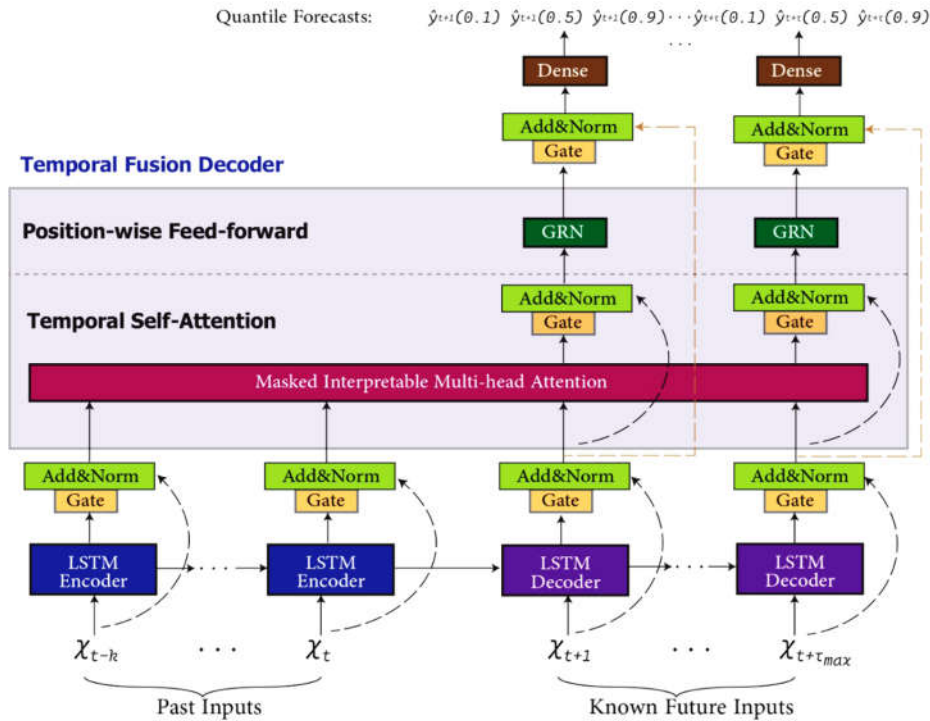$$GLU(X) = \sigma(W_1 X + b_1)\odot(W_2 X + b_2) \tag{3}$$

Figure 6. Structure of TFT (Ji et al. 2023).

Add&Norm denotes the integration of layer normalization and residual connection. This layer has demonstrated effectiveness in the extraction of features across a range of transformer structures. In addition, the gated residual network (GRN) is suggested to incorporate non-linear processing into the model selectively and when required. Equations (4) through (6) illustrate the GRN. LayerNorm() represents the normalization of a conventional layer. The GRN inputs are a and c; a was the principal input and c was the optional context vector. The function of Exponential Linear Unit (ELU), and $\beta_1 \in R^{d_{model}}$, $\beta_2 \in R^{d_{model}}$ are intermediate layers. W_3, W_4, W_5 are weight matrix parameters, while b_3, b_4 are the bias parameters Ji et al. (2023).

$$GRN(a, c) = LayerNorm(a + GLU(\beta_1)) \tag{4}$$

$$\beta_1 = W_3\beta_2 + b_3 \qquad\qquad (5)$$

$$\beta_2 = ELU(W_4\,a + W_5\,c + b_4) \qquad\qquad (6)$$

GRN enables the efficient transmission of data through the implementation of gating layers and skip connections. Like TFT are masked interpretable multi-head attention (MIMHA), excluding the GRN; by rectifying the multi-head attention (MHA), the TFT's attention is rendered simple and straightforward to comprehend. Consequently, the identical layers of MHA are implemented in the model; the original TFT contains additional information. As in TFT, a loss function called quantile loss was implemented. By utilizing these practical elements, the simplified variation of the TFT model remains effective for tasks involving forecasting. The MIMHA function improves a model's capability of focusing on distinct segments of the input series, thereby facilitating a greater comprehension and analysis of the TFT behaviors. This is accomplished by implementing a concealing technique and rendering the attention scores comprehensible. The formulation of the standard MHA is as follows:

$$Attention(Q,K,V) = softmax\left(\frac{QK^T}{\sqrt{d_k}}\right)V \qquad\qquad (7)$$

Where Q represents query, V denotes value matrices, K means key and d_k represents the dimension of keys. An M masking matrix is incorporated into the attention mechanism of the MIMHA to regulate the flow of information and improve the interpretability of the attention scores. The calculation for masked attention is given as follows, Fayer et al. (2023):

$$MaskedAttention(Q,K,V,M) = softmax\left(\frac{QK^T + M}{\sqrt{d_k}}\right)V \qquad\qquad (8)$$

To compel the Softmax function to produce values close to zero at specific positions, the masking matrix M is intentionally constructed with substantial negative values in areas where attention should be masked. As a result, the attention scores become more interpretable and the model can concentrate its efforts on the unmasked positions Ji et al. (2023). The hyperparameters utilized in the computational framework of the TFT model are outlined in Table 1, which provides a detailed overview of the model's configuration, including parameters that impact its performance and behavior. An instance of a hyperparameter is displayed in each row of the table, accompanied by its description that clarifies its function within the model and its default value.

Table 1. Hyperparameters of TFT.

PARAMETER	VALUE
Number of encoder layers	3
Number of decoder layers	32
Learning rate	0.001
Metrics	RMSE
Epochs	100
Context length	64
Batch size	64
Hidden dim	32
Number of heads	4
Dropout rate	0.1

3.4. Bayesian Optimization Algorithm for TFT Hyperparameter Tuning

Hyperparameter tuning refers to the iterative process of optimizing the hyperparameters of a model to maximize its performance on a validation dataset. In this research, the hyperparameters used in the TFT model are tuned by an algorithm called Bayesian optimization. Hyperparameters are essential elements in DL methodologies due to their substantial impact on the performance of DL models and their direct influence on the behavior of training algorithms. When searching for the optimal model configuration, BOA arises a practical and effective approach for resolving problems of function optimization that are widely present in computing. This methodology is especially well-suited for addressing problems involving functions that are related in nature and lack a closed analytical form. BOA has demonstrated its utility in tackling a range of challenges associated with functions, such as those that are highly computational, involve complex derivative evaluations, and involve non-convex functions El Ghazi and Aknin (2023). In the classification of texts, real-time prediction of multi-category and sentiment discrimination, BOA is frequently implemented. Concurrently, BOA is increasingly being applied to the prediction of sequential data Zhang et al. (2023). Enhancing the predictive accuracy of the model can be achieved with the optimal combination of hyperparameters; therefore, it is essential to optimize the model's hyperparameters. The parameter optimization function expression for BOA is represented in (9).

$$\chi \in argmax_{x \in \chi} f(y) \tag{9}$$

In (9), y represents the value to be optimized for the hyperparameter value. $f(y)$ is the performance function. Gaussian Process (GP) is used in the probabilistic agent model for BOA, a GP model is applied to the input space $y \in R$ in the presence of a particular objective function f.
Dataset D = $\{(y_1, z_1), (y_2, z_2,) \cdots (y_n, z_n)\}$, there are n samples, where $z_i = f(y_i)$. The GP probability model can subsequently be denoted as follows:

$$f \sim GP[\alpha(y), P(y, y')] \tag{10}$$

$\alpha(y)$ denotes the function's mean value, and α(y) = E[f(y)]. The function's mean value is usually set to 0. P (y, y′) represents a covariance function, for variable y, regarding the variable y, y′, P (y, y′) = Cov [f(y), f(y′)] exists Zhang et al. (2023).

BOA is applied in this research due to its efficiency and effectiveness in hyperparameter tuning, especially for complex models like the TFT. Traditional grid or random search methods can be time-consuming and computationally expensive, often failing to find the optimal combination of hyperparameters. However, BOA utilizes a probabilistic model to predict the performance of different hyperparameter settings and focuses on exploring the most promising configurations. This approach not only accelerates the tuning process but also enhances the model's prediction accuracy and generalization capabilities, making it particularly suitable for improving SOC estimation in EV batteries. Its ability to handle the high dimensionality and complex interactions of hyperparameters ensures that the TFT-BOA model achieves superior performance metrics with low RMSE, MAE, MSE, and MAPE values.

Model uncertainty in this problem was handled using the inherent capabilities of the TFT to capture both temporal patterns and probabilistic forecasts, combined with the BOA for hyperparameter tuning. The TFT's attention mechanisms and gating layers allow it to quantify uncertainty by learning the importance of different time series features and their temporal dependencies. Additionally, the BOA process inherently considers uncertainty in its probabilistic model, focusing on areas with higher uncertainty to improve model performance iteratively. This dual approach ensures that both the model's predictive accuracy and its ability to express uncertainty are optimized, leading to more reliable SOC predictions for EV batteries.

4. EXPERIMENTAL ANALYSIS

4.1. Experimental Setup

The experiments are performed in a system with 12 GB operating memory. The system is equipped with a CPU, Intel i5 CPU @3.2 GHz. The performance evaluation of this research was carried out using the BMW i3 electric vehicle Dataset. The TFT+BOA classification algorithm and the analysis of data are both performed with the help of the MATLAB module.

4.2. Performance Metrics

The efficiency of the TFT+BOA model is assessed using the subsequent metrics. RMSE, MAPE, MAE, and MSE as mentioned in the following formulas, were implemented as performance metrics by which the model's SoC estimation was assessed by Xiao et al. (2019) and Kumar et al. (2024):

$$RMSE = \sqrt{\frac{1}{N}\sum_{k=1}^{N}(SOC_k - SOC_k^*)^2} \tag{11}$$

$$MAE = \frac{1}{N}\sum_{k=1}^{N}(SOC_k - SOC_k^*) \tag{12}$$

$$MSE = \frac{1}{N}\sum_{k=1}^{N}(SOC_k - SOC_k^*)^2 \tag{13}$$

$$MAPE = \frac{1}{N}\sum_{k=1}^{N}\frac{(SOC_k - SOC_k^*)}{SOC_k} \tag{14}$$

4.3. Performance Evaluation

This section presents the evaluation of the proposed predictive model's comparative analysis. The data collected from the dataset are given as input to the predictive model. The data from the dataset are divided into test and training sets. According to these sets, the performance evaluation is performed with all the models. The performances of the TFT+BOA method in battery SoC prediction are measured based on various parameters like MAPE, MSE, MAE and RMSE.

Table 2. Proposed Model's Performances of SOC Estimation Under Varying Temperatures.

Temperature (∘C)	RMSE	MAE	MSE	MAPE
10	0.13	0.023	0.10	1.08
20	0.15	0.032	0.08	1.24
30	0.08	0.020	0.13	1.04
40	0.18	0.026	0.07	1.22
50	0.12	0.019	0.12	1.11
AVERAGE	0.13	0.024	0.10	1.13

As shown in Table 2, the proposed TFT+BOA model produces excellent SOC estimation results across a range of temperatures. The results indicate that all RMSEs are within 0.16%, MAEs are within 0.035%, MSEs are within 0.15%, and MAPEs are within 2%. The respective means of RMSE, MAE, MSE, and MAPE are 0.13, 0.024, 0.10, and 1.13. As a result, the proposed network demonstrates the ability to accurately estimate SOC values in the presence of varying temperatures by including the

influence of ambient temperature. Figure 7 shows the graphical plot of the proposed model RMSE parameter for SOC prediction under varying temperatures like 10, 20, 30, 40, and 50 degrees respectively. The RMSE values vary from a maximum of 0.18 to a minimum of 0.08. The obtained average RMSE is 0.13. Lower RMSE values indicate better accuracy in predicting SOC. RMSE values remain comparatively low despite minor fluctuations, indicating that the model generates accurate SoC predictions across a range of temperature settings.
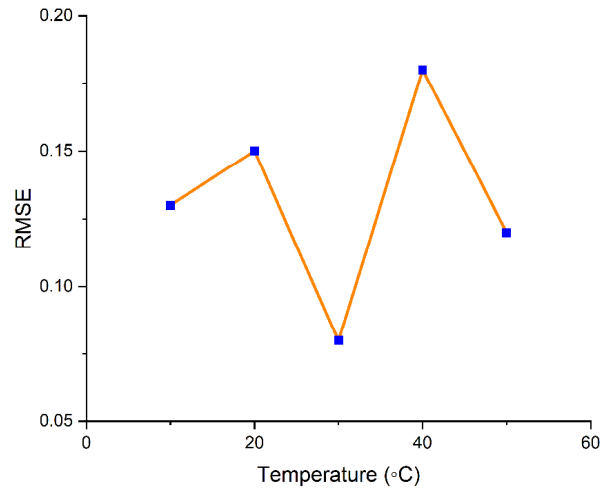
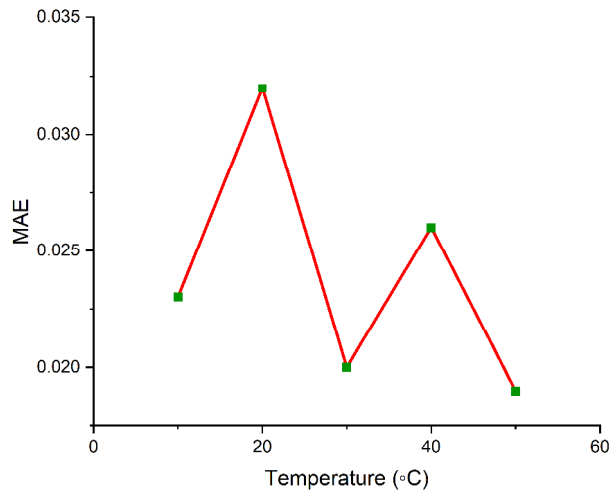Figure 7. Graphical Plot of RMSE Under Varying Temperatures.

Figure 8. Graphical Plot of MAE Under Varying Temperatures.

The graphical plot of MAE values under varying temperatures is shown in Figure 8. The MAE values vary from a maximum of 0.032 to a minimum of 0.019. the average value of 0.024 is obtained by the TFT+BOA model. The model consistently achieves low MAE values, which indicates its capability to generate accurate estimates of SoC despite variations in temperature. The average MAE value of 0.024 suggests that the model's predictions are consistently close to the true SoC values.
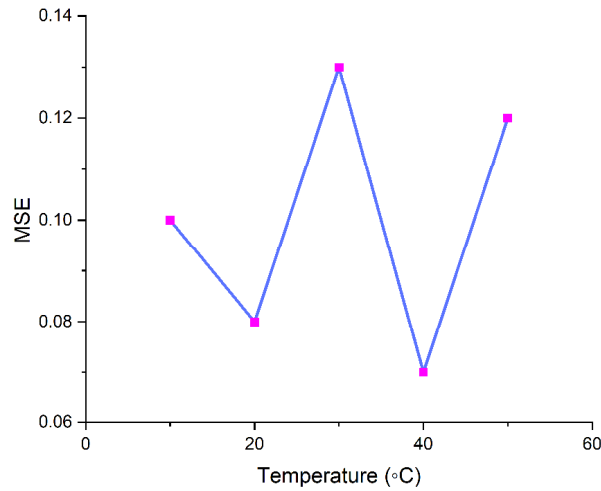

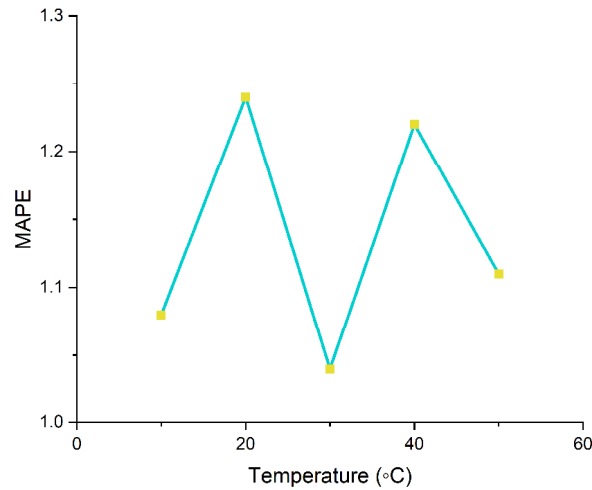Figure 9. Graphical Plot of MSE Under Varying Temperatures.

Figure 10. Graphical Plot of MAPE Under Varying Temperatures.

Figure 9 illustrates the MSE values of the proposed model under different temperature conditions. MSE vary from a maximum of 0.13 to a minimum of 0.07 with a difference of 0.06. Like RMSE and MAE, lower MSE values indicate better accuracy in predicting SOC. The model exhibits

consistent performance, as indicated by its comparatively low MSE values, which suggest that a significant proportion of predictions align closely with the true SoC values. Figure 10 illustrates the MAPE values of the proposed model under different temperature conditions. MAPE vary from a maximum of 1.24 to a minimum of 1.04 across various temperatures. Low MAPE values are consistently attained by the model, suggesting minimal error in the estimation of SOC. The narrow range of MAPE values across temperatures highlights the model's robustness in providing accurate SOC predictions regardless of temperature variations. A mean MAPE value of 1.13% validates the overall accuracy of the model in estimating SOC. Table 3 compares the proposed model's testing performance with existing models included in the review. The performance analysis was compared with models like LSSVM, GRU-RNN, NARXNN+LSA, TCN, LSTM+NARX, KALMAN FILTER, CNN-ESA, NARX-Net & ARIMA and LSTM. The proposed model produces better results compared to other models.

Table 3. Comparison of Performance Analysis.

MODEL	RMSE	MAE	MAPE	MSE
LSSVM (Li et al. 2020)	0.16	0.41	-	-
GRU-RNN (Xiao et al. 2019)	1.13	0.84	3.28	-
NARXNN+LSA (Lipu et al. 2018)	0.55	0.43	3.38	-
TCN (Liu et al. 2021)	0.87	0.67	-	-
LSTM+NARX (Wei et al. 2020)	0.78	0.69	1.24	-
KALMAN FILTER (Ling and Wei 2021)	0.48	0.41	-	-
CNN-ESA (Kumar et al. 2024)	-	0.075	2.65	0.152
NARX-Net & ARIMA (Khalid et al. 2019)	0.1707	0.0291	-	0.1383
LSTM (Wu et al. 2022)	0.453	0.343	-	0.206
PROPOSED MODEL TFT+BOA	0.13	0.024	1.13	0.10

Figure 11 shows the graphical plot for the comparison of RMSE values with various models. Based on the test performance comparison made with the existing models, the TFT-BOA model has a lower error rate than the other models. After comparing the models, it was determined that the Kalman Filter model has the smallest RMSE at 0.48, followed by the NARXNN+LSA model at 0.55. Models such as GRU-RNN and LSTM exhibit relatively higher RMSE values, indicating lower accuracy compared to the proposed model. The research model has an RMSE of 0.13, which is 1.13 to 0.16 lower than the other models.

Figure 12 shows the graphical plot for the comparison of values. The MAE value of the research model was 0.012, which is 1.14 to 0.016 lower than the compared models. The NARXNN+LSA model also demonstrates low MAE (0.43), followed by the Kalman Filter model (0.41). Greater MAE values are observed in models such as GRU-RNN and LSTM, which signifies the substantial differences between the predicted and observed values.

Figure 13 shows the graphical plot for the comparison of values. The MSE value of the research model was 0.10, which is 0.2 to 0.13 lower than the compared models. With an MSE of 0.10, the TFT+BOA model that has been proposed demonstrates an excellent level of overall accuracy in predicting SOC. Following the Kalman Filter model with an MSE of 0.206, the NARX-Net & ARIMA model attains the lowest MSE of 0.1383. Higher MSE values are observed in models like GRU-RNN and LSTM, indicating greater variations between the predicted and actual SOC values in comparison to the proposed model.
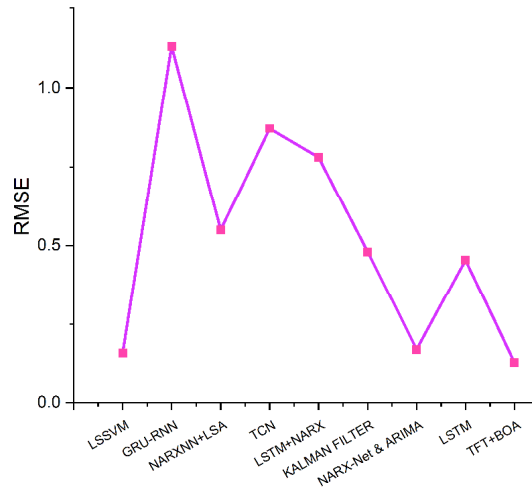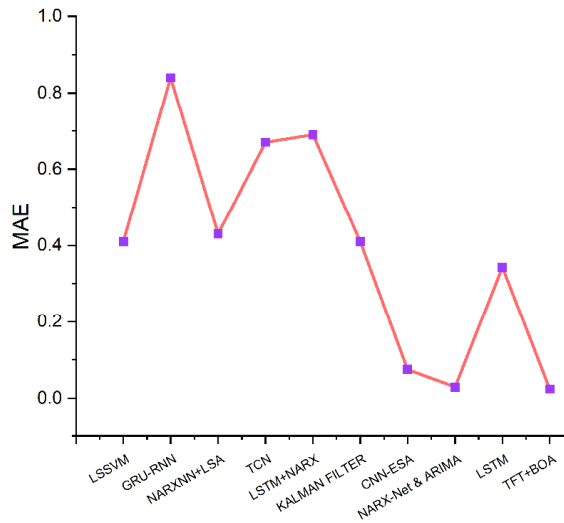
Figure 11. Graphical Plot of RMSE Comparison.

Figure 12. Graphical Plot of MAE Comparison.

Figure 14 shows the graphical plot for the comparison of values. The MAPE value of the research model was 1.13, which is 3.3 to 1.2 lower than the compared models. The CNN-ESA model exhibits the lowest MAPE of 2.65%, followed by the LSTM model with a MAPE of 1.24%. Other models, including NARXNN+LSA and NARX-Net & ARIMA, demonstrate higher MAPE values, suggesting larger percentage errors in SoC estimation compared to the proposed model. As a result, according to this comparison, the TFT+BOA model has obtained better results than the compared models in this research. The TFT-BOA model generates accurate results for SOC estimation, as evidenced by low values of RMSE, MAE, MSE, and MAPE. Hyperparameter tuning ensures that the

model is fine-tuned to the specific characteristics of the dataset, leading to improved accuracy and generalization. The TFT-BOA model outperforms various existing models for SOC prediction, including LSSVM, GRU-RNN, NARXNN+LSA, TCN, LSTM+NARX, Kalman Filter, CNN-ESA, NARX-Net & ARIMA, as demonstrated by the comparative analysis. This highlights the proposed model's superiority in terms of accuracy and performance under different temperatures. The TFT-BOA model may require significant computational resources, especially during hyperparameter tuning and training phases. Integrating the TFT-BOA model into real-time battery management systems may pose practical challenges, including latency issues, resource constraints, and the need for continuous model updates. Addressing these challenges would be crucial for ensuring the practical applicability of the model in dynamic operational environments.
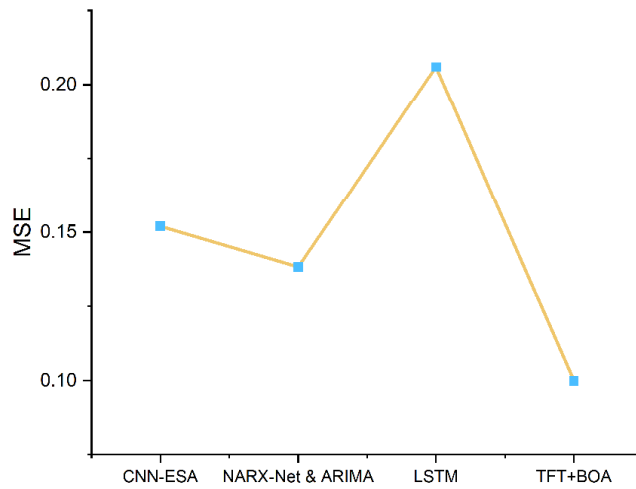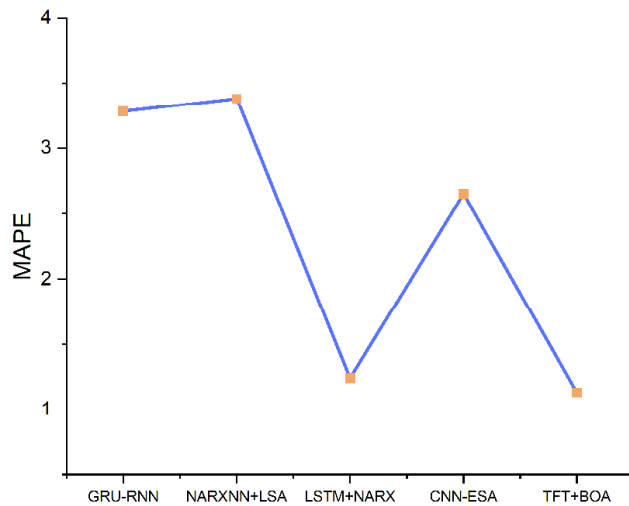

Figure 13. Graphical Plot of MSE Comparison.

Figure 14. Graphical Plot of MAPE Comparison.

5. CONCLUSION

In this paper, a combined TFT-BOA model for the SOC estimation of LIBs was proposed. The research model has a series of workflows including data pre-processing, feature extraction, classification and hyperparameter tuning. Data collected from the dataset are preprocessed by min-max normalization. Extraction of features from the preprocessed data and classification is done by the TFT algorithm. The hyperparameters of TFT were tuned by using a Bayesian Optimization Algorithm. The data set was partitioned for training and evaluating the proposed model. TFT-BOA model performance was assessed by the SOC parameters such as RMSE, MAE, MSE and MAPE. The proposed model generates accurate results, with all RMSEs below 0.16%, MAEs below 0.035%, MSEs below 0.15%, and MAPEs within 2%. The average values of RMSE, MAE, MSE, and MAPE are 0.13, 0.024, 0.10, and 1.13 respectively. The proposed results are compared with the various models like LSSVM, GRU-RNN, NARXNN+LSA, TCN, LSTM+NARX, KALMAN FILTER, CNN-ESA, NARX-Net & ARIMA and LSTM. The comparative analysis shows that the proposed TFT+BOA model was the best method for SOC prediction under different temperatures, with minimum error values of RMSE, MAE, MSE and MAPE. In conclusion, the proposed SOC estimation method for LIBs, which is based on the TFT-BOA, has been rigorously validated and has yielded excellent results. To assure practical applicability in dynamic operational environments, future implementation of the proposed model into real-time battery management systems may necessitate consideration of delay and limitations on resources.

Nomenclature	
BMS	Battery Management System
BMW	Bayerische Motoren Werke
BOA	Bayesian Optimization Algorithm
CAGR	Compound Annual Growth Rates
CO_2	Carbon-di-oxide
CV	Cross Validation
CNN	Convolutional Neural Network
DL	Deep Learning
DST	Dynamic Stress Test
E-CNN	Extended Convolutional Neural Network
EKF	Extended Kalman Filter
ELU	Exponential Linear Unit
EO	Equilibrium Optimization
ESA	Elephant Search Algorithm

EV	Electric Vehicle
FOM	Fractional-Order Model
GRN	Gated Residual Network
GRU	Gated Recurrent Unit
GWO	Grey Wolf Optimization
LIB	Lithium Ion Battery
LSA	Lighting Search Algorithm
LSSVM	Least Squares Support Vector Machine
LSTM	Long Short-Term Memory
ML	Machine Learning
MAE	Mean Absolute Error
MAPE	Mean Absolute Percentage Error
MIMHA	Masked Interpretable Multi-Head Attention
MSE	Mean Squared Error
NARX	Nonlinear Autoregressive with External input
NARXNN	Non-linear Autoregressive Network with Exogenous Inputs Neural Network
PSO	Particle Swarm Optimization
RMSE	Root Mean Squared Error
RNN	Recurrent Neural Network
SOC	State of Charge
SoH	State of Health
SRNN	Stacked Recurrent Neural Network
TFT	Temporal Fusion Transformer
UDDS	Urban Dynamometer Driving Schedule
USD	United States Dollars

References

Chang M., Bae S., Cha G., and Yoo J., Aggregated Electric Vehicles fast-charging power demands analysis and forecasts based on LSTM neural networks, Sustainability, vol. 13, no. 24, 2021.

Chen Y. et al., A review of lithium-ion battery safety concern: The issue, strategies, and testing standard, Journal of Energy Chemistry, vol. 59, pp. 83-99, 2020.

El Ghazi M. and Aknin N., Optimizing Deep LSTM Models through Hyperparameters Tuning for Sensors-Based Human Activity Recognitions in Smart Homes, Informatica, vol. 47, no. 10, pp. 109–122, 2023.

Fayer G. et al., A temporal fusions transformers deep learning model for long-term streamflow forecasting: a case study in the funil reservoirs, Southeast Brazil, Knowledge-Based Engineering and Science, vol. 4, no. 2, pp. 73-88, 2023.

Habib A. K. M. A. et al., Lithium-ion battery managements systems for electric vehicle: constraint, challenge, and recommendation, Batteries, vol. 9, no. 3, 2023.

Huang S. C. et al., An online SOC and SOH estimations model for lithium-ion batteries, Energies, vol. 10, no. 4, 2017.

Ji W., Cao Z., and Li X., Multi-Tasks Learning and Temporal-Fusions-Transformers-Based Forecasting of Building Power Consumptions, Electronics, vol. 12, no. 22, 2023.

Jin S. et al., Overview of machine learning method for lithium-ion battery remaining useful lifetime predictions, Electronics, vol. 10, no. 24, 2021.

Khalid A. et al., A multi-steps predictive model to estimate li-ion states of charges for higher c-rate, IEEE International Conferences on Environments and Electrical Engineering and 2019 IEEE Industrials and Commercial Power System, Europe, 2019.

Kumar I., Dasari M., Danamaraju C., Bindu K. V., Mohanavel V., and Dhanraj J. A., Improving State of Charge Estimation for Lithium-Ion Batteries through Optimized CNN Models, In 2024 5th International Conference on Mobile Computing and Sustainable Informatics, pp. 519-524, 2024.

Li J. et al., A novel state of charge approach of lithium-ion battery using least square support vector machines, IEEE Access, vol. 8, pp.195398-195410, 2020.

Ling L. and Wei Y., State-of-charges and state-of-health estimations for lithium-ion batteries based on dual fractional-orders extended Kalman filters and online parameters identifications, IEEE Access, vol. 9, pp. 47588-47602, 2021.

Lipu M. S. H. et al., State of charges estimations for lithium-ion battery using recurrent NARX neural networks model-based lighting search algorithms, IEEE Access, vol. 6, pp. 28150-28161, 2018.

Lipu M. S. H. et al., State of charges estimations in lithium-ion batteries: A neural network optimization approach, Electronics, vol. 9, no. 9, 2020.

Liu Y., Li J., Zhang G., Hua B., and Xiong N., State of charges estimations of lithium-ion batteries based on temporal convolutional networks and transfer learning, IEEE Access, vol. 9, pp. 34177-34187, 2021.

Liu Z. et al., A DDoS Detections Method Based on Features Engineering and Machine Learning in Software-Defined Network, Sensors, vol. 23, no. 13, 2023.

Meng J. et al., Overview of lithium-ion battery modelling method for state-of-charges estimations in electrical vehicle, Applied sciences, vol. 8, no. 5, 2018.

Miao Y., Hynan P., Jouanne A. V., and Yokochi A., Current Li-ion battery technologies in electric vehicle and opportunities for advancement, Energies, vol. 12, no. 6, 2019.

Mo T., Li Y., Lau K., Poon C. K., Wu Y., and Luo Y., Trend and Emerging Technologies for the developments of electric vehicle, Energies, vol. 15, no. 17, 2022.

Pevec D., Babic J., and Podobnik V., Electric vehicle: A data science perspective review, Electronics, vol. 8, no. 10, 2019.

Rajper S. Z. and Albrecht J., Prospect of electric vehicle in the developing countries: A literature review, Sustainability, vol. 12, no. 5, 2020.

Rangarajan S. S. et al., Lithium-ion batteries—The crux of electric vehicle with opportunities and challenge, Clean Technologies, vol. 4, no. 4, pp. 908-930, 2022.

Renold A. P. and Kathayat N. S., Comprehensive Review of Machine Learning, Deep Learning, and Digital Twin Data-Driven Approaches in Battery Health Predictions of Electric Vehicle, IEEE Access, vol. 12, pp. 43984-43999, 2024.

Rivera-Barrera J. P., Muñoz-Galeano N., and Sarmiento-Maldonado H. O., SoC estimations for lithium-ion batteries: Review and future challenge, Electronics, vol. 6, no. 4, 2017.

Saldana G., J. San Martín I., Zamora I., Asensio F. J., and Onederra O., Analysis of the current electric battery model for electric vehicles simulations, Energies, vol. 12, no. 14, 2019.

Sanguesa J. A., Torres-Sanz V., Garrido P., Martinez F. J., and Marquez-Barja J. M., A review on electric vehicle: Technologies and challenge, Smart Cities, vol. 4, no. 1, pp. 372-404, 2021.

Sharma P. and Bora B. J., A review of modern machine learning technique in the predictions of remaining useful life of lithium-ion batteries, Batteries, vol. 9, no. 1, 2022.

Sherkatghanad Z., Ghazanfari A., and Makarenkov V., A self-attention-based CNN-Bi-LSTM model for accurate state-of-charges estimations of lithium-ion batteries, Journal of Energy Storage, vol. 88, 2024.

Stampatori D. et al., Li-ion batteries: A review of a key technology for transports decarbonizations, Energies, vol. 13, no. 10, 2020.

Sulaiman M. H. and Mustaffa Z., State of Charges Estimations for Electric Vehicle Using Random Forests, Green Energy and Intelligent Transportations, vol. 9, pp. 47588-47602, 2024.

Sun X. et al., Technology developments of electric vehicle: A review, Energies, vol. 13, no. 1, 2019.

Thangavel S., Mohanraj D., Girijaprasanna T., Raju S., Dhanamjayulu C., and Muyeen S. M., A comprehensive review on electric vehicles: battery managements systems, charging stations, traction motor, Energies, vol. 1, pp. 20994-21019, 2023.

Vakharia V. et al., Estimations of lithium-ion battery discharges capacity by integrating optimized explainable-AI and stacked LSTM models, Batteries, vol. 9, no. 2, 2023.

Wei Y M., Ye M., Li J. B., Wang Q., and Xu X., State of charges estimations of lithium-ion batteries using LSTM and NARX neural network, IEEE Access, vol. 8, pp. 189236-189245, 2020.

Wu X., Li M., Du J., and Hu F., SOC predictions methods based on battery packs aging and consistency deviations of thermoelectric characteristics, Energy Reports, vol. 8, pp. 2262-2272, 2022.

Xiao B., Liu Y., and Xiao B., Accurate state-of-charges estimations approach for lithium-ion batteries by gated recurrent units with ensemble optimizers, IEEE Access, vol. 7, pp. 54192-54202, 2019.

Zhang D., Jin X., Shi P., and Chew X. Y., Real-time loads forecasting models for the smart grids using Bayesian optimized CNN-BiLSTM, Frontiers in Energy Research, vol. 11, 2023.

Zhang D., Zhong C., Xu P., and Tian Y., Deep learning in the state of charges estimations for li-ion batteries of electric vehicle: A review, Machines, vol. 10, no. 10, 2022.

Zhang M. and Fan X., Review on the state of charges estimations method for the electric vehicle battery, World Electric Vehicle Journal, vol. 11, no. 1, 2020.

Zhang R. et al., State of the arts of lithium-ion battery SOC estimations for electrical vehicle, Energies, vol. 11, no. 7, 2018.

Zhao F., Li Y., Wang X., Bai L., and Liu T., Lithium-ion batteries state of charges predictions of electric vehicle using RNN-CNN neural network, IEEE Access, vol. 8, pp. 98168-98180, 2020.